Inorganic Chemistry
Article
Cite This: Inorg. Chem. XXXX, XXX, XXX−XXX
pubs.acs.org/IC

Interplay of Coordination Environment and Magnetic Behavior of Layered Co(II) Hydroxichlorides: A DFT+U Study

Diego Hunt,*[,†] Matías Jobbagy,[‡] and Damián A. Scherlis*[,‡]

[†]Departamento de Física de la Materia Condensada, GIyA, CACCNEA, Instituto de Nanociencia y Nanotecnología, CNEA-CONICET, 1650 San Martin, B1650 Buenos Aires, Argentina

[‡]Departamento de Química Inorgánica, Analítica y Química Física/INQUIMAE, Facultad de Ciencias Exactas y Naturales, Universidad de Buenos Aires, Ciudad Universitaria, Pab. II, Buenos Aires C1428EHA, Argentina

Supporting Information

ABSTRACT: In this work we present a systematic computational study of the structural and magnetic properties of a layered family of Co(II) hydroxichlorides, obeying to the general formula $Co(OH)_{2-x}Cl_x(H_2O)_y$. This solid contains both octahedral and tetrahedral cobalt ions, displaying a complex magnetic order arising from the particular coupling between the two kinds of metallic centers. Here, supercells representing concentrations of 12, 20, and 40% of tetrahedral sites were modeled consistently with the compositions reported experimentally. Our simulations show that the two types of cobalt ions tend to couple antiferromagnetically, giving rise to a net magnetic moment slightly out of the plane of the layers. The band gap reaches its minimum value of 1.4 eV for the most diluted fraction of tetrahedral Co(II) sites, going up to 2.2 eV when the content is 40%. Moreover, our results suggest that the presence of interlayer water stabilizes the material and at the same time strongly modifies the electronic environment of tetrahedral Co(II), leading to a further drop of the band gap. To our knowledge, this is the first theoretical investigation of this material.

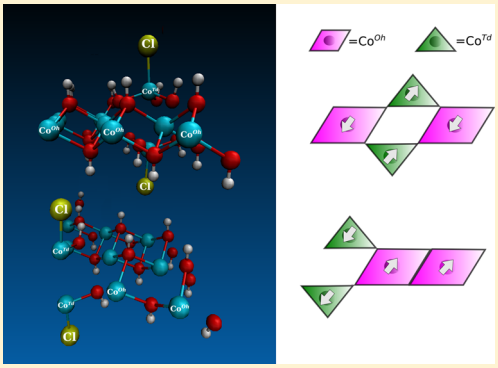

INTRODUCTION

In contrast to other divalent transition metals, cobalt(II) can adopt several coordination environments, including octahedral, tetrahedral, square-pyramidal, trigonal-bipyramid, and square-planar configurations, and hence its crystalline phases exhibit an extremely rich variety of structures.[1−3] This exceptional versatility results in a vast family of crystalline arrays, ranging from simple quasi-two-dimensional (2-D) hydroxides or basic salt layered materials[4,5] to complex three-dimensional metal−organic frameworks.[1] Among the former phases, the family of layered basic salts known as α-Co(II) hydroxides caught particular attention since the report of an improved method of synthesis, either in the form of strictly inorganic basic salts[6] or intercalated with large organic spacers.[5,7,8] This phase contains a predominant fraction of octahedral Co(II) centers, hereafter denoted as Co^{Oh}, which display a brucitic hexagonal arrange.[9] Certain Co^{Oh} positions of each layer are vacant, and these sites are occupied by a pair of tetrahedral Co(II) centers, Co^{Td}, positioned externally to the hydroxilated layer. This structural configuration, bearing the ideal formula $Co^{Oh}_{0.828}Co^{Td}_{0.348}(OH)_2(Cl)_{0.348}0.46H_2O$, results in an interbasal distance [003] of 8.02 Å (c = 24.058 Å cell parameter), significantly expanded with respect to the [001] distance of 4.653 Å observed for brucitic β-$Co(OH)_2$.[9] This phase, at variance with the well-defined mineral parent structure of simonkolleite,[10] $Zn^{Oh}_3Zn^{Td}_2(OH)_8Cl_2{\cdot}nH_2O$, exhibits a disordered distribution of Co^{Td} sites within the layers.

Shortly after the accurate characterization of the α phase, alternative synthetic, kinetically controlled procedures allowed for the modulation of the Co^{Oh} to Co^{Td} ratio, giving birth to a family of Co-layered hydroxides obeying to the general formula $Co^{Oh}_{1-x}Co^{Td}_x(OH)_{2-x}(Cl)_x.yH_2O$, with $0.26 \leq x \leq 0.5$.[11] Bragg profiles and pair distribution functions from scattering experiments have been used to elucidate the structures of partially ordered systems including nanoparticles and layered materials.[12−14] Neilson and collaborators employed these methods to interpret the short order distribution of metal centers and to resolve the intralayer structure of different cobalt hydroxides, revealing the nature of metal site coordination.[15] Nevertheless, the distribution of Co^{Td} within the layer and the kind of magnetic interactions between the two types of Co(II) are currently under discussion. Interestingly, this phase develops without a significant distortion of the intralayer Co(II)−Co(II) distance or coordination environment, arising as a close to ideal model to probe the incidence of Co^{Td} abundance and spatial distribution on the magnetic and electronic properties of these solids. In the present work, we explored the magnetic coupling and structural features of a

Received: December 28, 2017

DOI: 10.1021/acs.inorgchem.7b03231
Inorg. Chem. XXXX, XXX, XXX−XXX

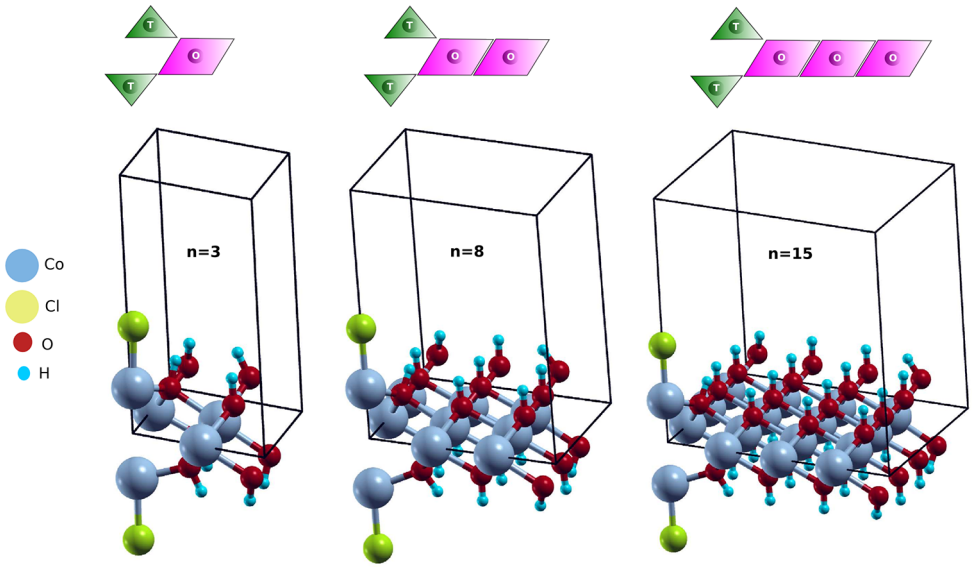

Figure 1. Schematic view of the supercells employed to model the α hydroxide layers. In the top panel, green triangles represent the location of Co^{Td} ions, while magenta rhombi represent Co^{Oh} ones. Yellow spheres denote chloride anions coordinated to Co^{Td}.

series of representative α cobalt hydroxides by means of DFT +U simulations, employing reduced supercells. To the best of our knowledge, this one is the first theoretical report on the magnetic and structural properties of α hydroxides cobalt phases.

METHODS

DFT Calculations. All calculations were performed employing density functional theory (DFT) as implemented in the Quantum Espresso code,[16] which is based on the pseudopotential approximation to represent the ion−electron interactions, and plane waves basis sets to expand the Kohn−Sham orbitals. Ultrasoft type pseudopotentials were adopted, in combination with the PBE formalism to compute the exchange−correlation term.[17] The incidence of the Hubbard parameter in the DFT+U calculations on the magnetic coupling and other properties was explored by screening its value between 3 and 7.8 eV, based on previous reports.[18−22] An energy threshold of 10^{-8} au was used for self-consistency, while for geometry optimization, the convergence criteria were 10^{-6} au for the energy and of 10^{-3} au for the forces per atom. To improve the numerical convergence, in particular for pure DFT calculations for which the system becomes metallic, a first-order Methfessel−Paxton spreading was implemented. van der Waals interactions were considered by including the semiempirical correction DFT-D originally introduced by Grimme[23] and implemented in a plane-wave framework by Barone and co-workers.[24]

Supercells. The simulations were carried out on supercells with specific ordering of the metal polyhedra within the layer and a general formula $[Co^{Oh}{}_nCo^{Td}{}_2(OH)_{2n+2}Cl_2]_m\cdot(H_2O)_{y\cdot m}$, according to the representative arrays characterized by Nielsen et al.,[15] where n = 3, 8 and 15, m represents the number of layers, and y the number of water molecules per layer (Figure 1). In the following, the aforementioned supercells will be referred to as $[Co^{Oh}{}_3Co^{Td}{}_2(OH)_8Cl_2]$, $[Co^{Oh}{}_8Co^{Td}{}_2(OH)_{18}Cl_2]$, and $[Co^{Oh}{}_{15}Co^{Td}{}_2(OH)_{32}Cl_2]$. These model cells represent a concentration of tetrahedral cobalt centers of 40, 20, and 12%, respectively, in line with observed chemical compositions.[9,25]

Brillouin zone sampling was performed on these supercells with a Monkhorst−Pack grid, checking for convergence with respect to the number of k-points. In the case of $[Co^{Oh}{}_3Co^{Td}{}_2(OH)_8Cl_2]$ supercells, parameters $a = b$ = 6.23 Å and c = 18.7 Å were adopted, based on experimental data, employing a 3 × 3 × 1 k-point mesh. The same mesh was used in the case of $[Co^{Oh}{}_8Co^{Td}{}_2(OH)_{18}Cl_2]$, with supercell parameters $a = b$ = 9.35 Å and c = 18.7 Å (isolated layer). Finally, for the largest model with 12% of tetrahedral cobalt, $[Co^{Oh}{}_{15}Co^{Td}{}_2(OH)_{32}Cl_2]$, with cell parameters $a = b$ = 12.48 Å and c = 18.7 Å (isolated layer), a 2 × 2 × 1 k-point grid was used. To evaluate the interlayer magnetic coupling, supercells containing two layers were built by properly stacking the bidimensional arrays; interlaminar water molecules were taken into account in all cases.

RESULTS AND DISCUSSION

The incorporation of a Hubbard term in the Kohn−Sham Hamiltonian that penalizes on-site electron interactions and inhibits d-charge delocalization has proven effective to correct the well-known DFT deficiencies to describe the electronic properties of transition metal oxides.[26−28] In particular, the use of a Hubbard parameter U allows to properly reproduce the magnetic behavior of cobalt oxides and hydroxides, including the α phases. DFT+U calculations have been applied to investigate the structural and magnetic behavior of CoO[20] and Co_3O_4[21] crystals. In these cases, the effect of the U parameter was screened within an ample range of values. Our own experience on this family of cobalt compounds shows that, while the choice of U may determine the exact value of energetic differences, it does not lead to inversions in the relative stability of the accessible states.[29] This is in fact also the case for the present system, as it will be discussed later in this section. Then, unless indicated explicitly, and on the basis of our previous simulations,[29] all calculations presented in this study were performed with U = 4.5.

In related compounds containing both octahedral and tetrahedral cobalt, the experimental analysis typically indicates that the coupling is ferromagnetic between the sites of the same kind and antiferromagnetic between sites of a different nature, with the spin moment lying in-plane (see e.g. ref 5). In recent experimental work on β-$Co(OH)_2$, we found that the magnetic refinement of the β phase was in principle consistent with a spin orientation parallel to the layers.[29] Such a configuration actually reproduced the main features of the magnetic diffraction pattern. However, the agreement between the diffraction pattern and the Rietveld refinement could be further increased by introducing an out-of-plane component of the magnetic moment, subtending an angle θ of 57.9° with respect

DOI: 10.1021/acs.inorgchem.7b03231
Inorg. Chem. XXXX, XXX, XXX−XXX

to the z-axis[29] (where a value of $\theta = 90°$ corresponds to the spins parallel to the sheet lying on the xy-plane). This slightly out-of-plane alignment was coincident with the angle predicted from DFT+U calculations,[29] and it seems to be also present in the α phase, as shown in Figure 2, which explores the effect of

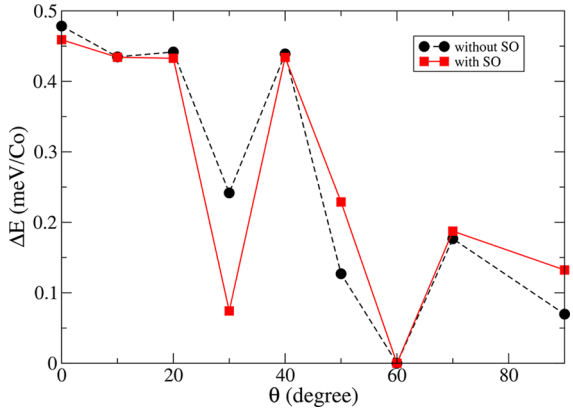

Figure 2. Relative stability of the ground state of an isolated layer (where Co^{Oh} and Co^{Td} are antiferromagnetically coupled), in meV/Co, as a function of the magnetization angle, θ. Values of $\theta = 0$ and 90° correspond to the spins oriented orthogonal (z-polarized) and parallel to the layer, respectively.

the magnetization angle θ on the energy of the antiferromagnetic state. The curve exhibits a global minimum at $\theta = 60°$, almost the same angle as that found for β-$Co(OH)_2$, which is in turn coincident with the direction of the Co−O bonds.[29] The spin−orbit contribution does not have a significant effect on the shape of the curve, with no incidence in the value of the θ angle. This result is consistent with the invariance of the product between the magnetic susceptibility and the temperature (χ_MT) with respect to the spin−orbit parameter reported for cobalt(II) complexes at low T.[30] Figure 2 reflects a magnetic anisotropy characteristic of cobalt compounds.[2,3] Thus, unless indicated explicitly, all calculations presented henceforth have been performed with $\theta = 60°$.

Table 1 presents the energy difference between the antiferromagnetic (AF) and ferromagnetic (FM) states

Table 1. Energy of the FM Configuration Relative to the Ground (AF) State, in meV/Co, for a Single Hydroxide Layer with Different Proportions of Tetrahedral Cobalt Sites

magnetic state	ΔE/Co (n = 3)	ΔE/Co (n = 8)	ΔE/Co (n = 15)
FM	23	11	6

corresponding to the arrangements displayed in Figure 3 for the $n = 3$ cell (the configurations for $n = 8$ and 15 are presented

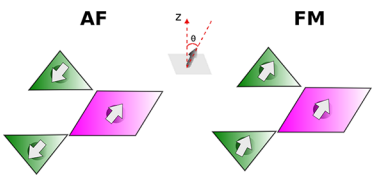

Figure 3. Schematic representation of AF and FM states of Co(II) for a supercell with $n = 3$. The two kinds of coordination environments, tetrahedral and octahedral, are represented in different colors as in Figure 1.

in the SI). According to DFT+U, in the ground state the magnetic moments of the Co^{Oh} sites are anti-aligned with respect to those of Co^{Td}; the magnitude of the total magnetization of one layer depends on the n value, being 3, 18, and 39 μB, for n = 3, 8, and 15, respectively.[31]

This kind of interaction can be understood in terms of a superexchange mechanism between cobalt ions, where the O atoms of the OH bridges play the role of the non-magnetic ligand, and the bond adopts a geometry consistent with the Goodenough−Kanamori rules.[32] These rules predict a strong antiferromagnetic coupling when the angle formed by the magnetic centers with the ligand in between is close to 180°, with a partially filled d shell. A weak ferromagnetism is expected, on the other hand, for angles close to 90°. In the present case the Co^{Td}−OH−Co^{Oh} angle is 119.89° ,while the value of the Co^{Oh}−OH−Co^{Oh} angle is 97.58°. In a similar way, the nature of magnetic interactions can be interpreted from the Kahn's model:[33] The orthogonality of the magnetic orbitals between octahedral Co(II), with angles close to 90°, favors the ferromagnetic interactions. On the other hand, the Co^{Td}−OH−Co^{Oh} angle, being bigger than 90°, leads to a non-orthogonal geometry and the consequent antiferromagnetic coupling (see SI). The optimized structural parameters corresponding to the three isolated supercells are shown in Table 2. The lattice distance d_{110}, which represents the intralayer metal−metal distance and the interatomic lengths, are in good agreement with the experimental results obtained by Neilson et al. by means of Rietveld refinement.[25]

The magnitudes of the magnetic couplings constants between octahedral sites (J_O), and between Co^{Oh} and Co^{Td} (J_T), were estimated from the parametrization of a isotropic Heisenberg Hamiltonian with nearest-neighbor interactions. The details can be found in the Supporting Information. The results, summarized in Table 3, show that the magnitudes of both kinds of magnetic couplings increase together with the molar fraction of tetrahedral cobalt. The comprehensive analysis of Kurmoo of several related phases concluded that there is a linear relationship between the critical temperature T_c and the Co^{Td} molar fraction for highly hydroxilated layered cobalt compounds.[1] Underlying this behavior, a direct proportionality between the magnitude of the magnetic interaction and the critical temperature was identified. Noticeably, this experimental observation is in line with the trend revealed by our simulations. The reason behind this increase in J is not evident at all. In principle it could be attributed to the geometry, since the Co^{Oh}−OH−Co^{Oh} angle tends to decrease with the concentration of tetrahedral sites, while the Co−OH bond lengths are smaller for n = 3 (see Table 2). However, at the same time the Co^{Oh}−OH−Co^{Td} angle experiences a small increase.

Figures 4 and 5 depict, respectively, the band structure and the density of states for n = 3. A direct band gap of approximately 2.2 eV at Γ point is observed. An inspection around the Fermi level shows that the dominant contributions to the valence band arise from p orbitals of oxygen and chlorine atoms. The conduction band reflects a strong presence of the d orbitals of Co^{Oh} and Co^{Td}. Moreover, the d orbitals show a double degeneration splitting: d_{zx}/d_{zy} and $d_{x^2-y^2}/d_{xy}$; this degeneration is characteristic of trigonal pyramid geometries. In the present case a distortion results from the inherently larger Co^{Td}−Cl distance with respect to the Co^{Td}−OH length, allowing for an independent electronic behavior of the d_{z^2} orbital, compared to the remnant d counterpart. An analogous

DOI: 10.1021/acs.inorgchem.7b03231
Inorg. Chem. XXXX, XXX, XXX−XXX

Table 2. Optimized Lattice Parameters, in Å, for a Single Hydroxide Layer with Different Molar Fractions of Tetrahedral Cobalt[a]

n	d_{110}	Co^{Oh}–OH	Co^{Td}–OH	Co^{Td}–Cl	γ	λ
3	3.134	2.062	1.857	2.27	97.6	119.9
8	3.142	2.108	1.862	2.326	97.9	120.4
15	3.138	2.071	1.861	2.25	98.0	121.2
exp ($n \approx 8$)	3.14048	2.124	1.898	2.32	–	–

[a]The experimental values were obtained from Rietveld refinements[9] and correspond to $n \approx 8$. γ and λ represent the Co^{Oh}–OH–Co^{Oh} and Co^{Oh}–OH–Co^{Td} angles (in degrees), respectively.

Table 3. Magnetic Coupling Constants, in meV, for Different Molar Fractions of Tetrahedral Cobalt Ions[a]

n	J_T	J_O
3	−0.85	2.56
8	−0.40	0.19
15	−0.22	0.04

[a]J_T and J_O represent Co^{Oh}–Co^{Td} and Co^{Oh}–Co^{Oh} interactions, respectively.

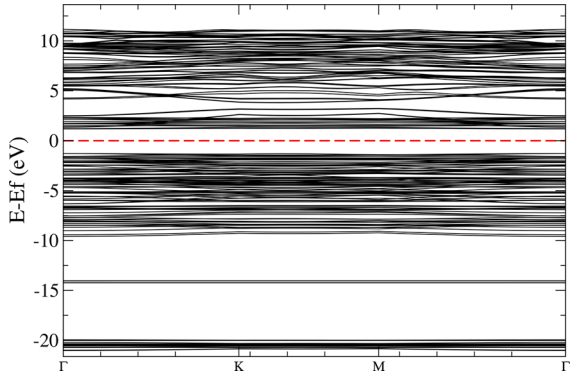

Figure 4. Band structure calculated for a single layer of $[Co^{Oh}{}_3Co^{Td}{}_2(OH)_8Cl_2]$ along the $\Gamma \rightarrow K \rightarrow M \rightarrow \Gamma$ directions.

behavior is observed in the other supercells. The band gap values (E_{gap}) obtained for the different supercells simulated herein are summarized in Figure 6. These values are represented as a function of the relative abundance of octahedral sites, expressed as the Co^{Oh} molar fraction, X_{Oh}. Curiously, E_{gap} does not follow a monotonic behavior with the concentration of octahedral cobalt. It drops from around 2.2 eV for $n = 3$ to almost 1.4 eV for $n = 15$, but it goes back to 2 eV when the fraction of Co^{Oh} reaches 1. The projected and total density of states for $n = 8$ and $n = 15$ supercells in Figure 7 show that with the increment of Co^{Td} sites, the p states of Cl

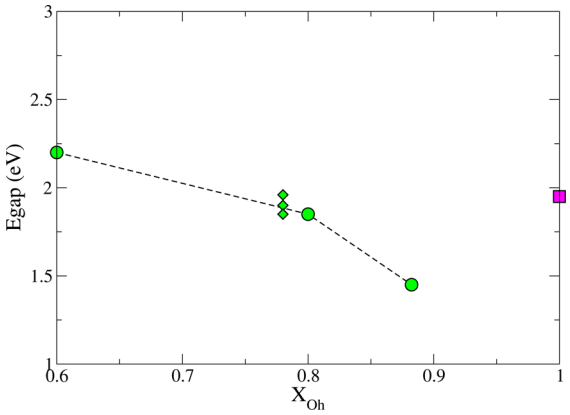

Figure 6. E_{gap} calculated by DFT+U as a function of Co^{Oh} cobalt molar fraction, X_{Oh}, for a single layer of the α-hydroxide. Green circles correspond to the α phase with $n = 3$, 8, and 15, whereas green rhombi refer the values obtained for the different arrays with $n = 14$. The pink square depicts the band gap value reported for the β phase.

atoms and the d orbitals of tetrahedral cobalt cations have a larger contribution to both the valence and conduction bands. On the other hand, the increase in the concentration of octahedral sites gives rise to a greater contribution of the p orbitals of O atoms in the vicinity of the Fermi level. The combination of these two ingredients results in this particular behavior where the minimum gap is seen for an intermediate content of tetrahedral sites.

The intrinsic disorder in the position of Co^{Td} inside the sheet does not seem to affect the magnetic ordering. Relative energies for different distributions of the tetrahedral ion in supercells with $n = 14$ were computed (see SI) to find that the most stable state corresponds to a given array of Co^{Td} in which the distance between tetrahedral sites is approximately 5.4 Å. This arrangement minimizes the electronic repulsion between the chlorides. These data are included in Figure 6. Beyond this, in

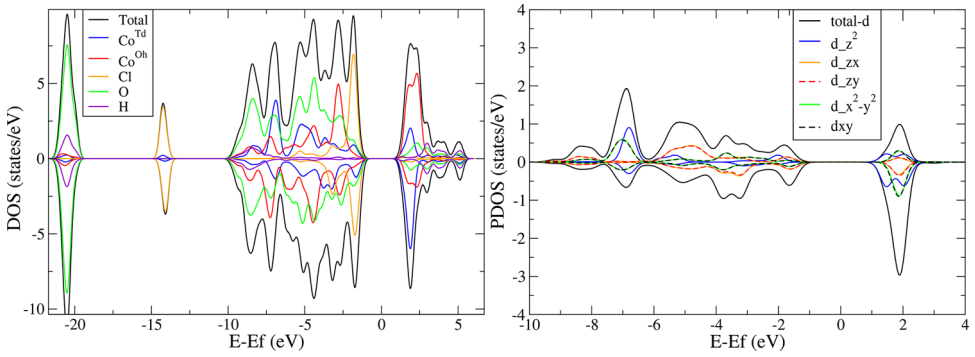

Figure 5. Total and projected density of states for a single layer of $[Co^{Oh}{}_3Co^{Td}{}_2(OH)_8Cl_2]$.

DOI: 10.1021/acs.inorgchem.7b03231
Inorg. Chem. XXXX, XXX, XXX–XXX

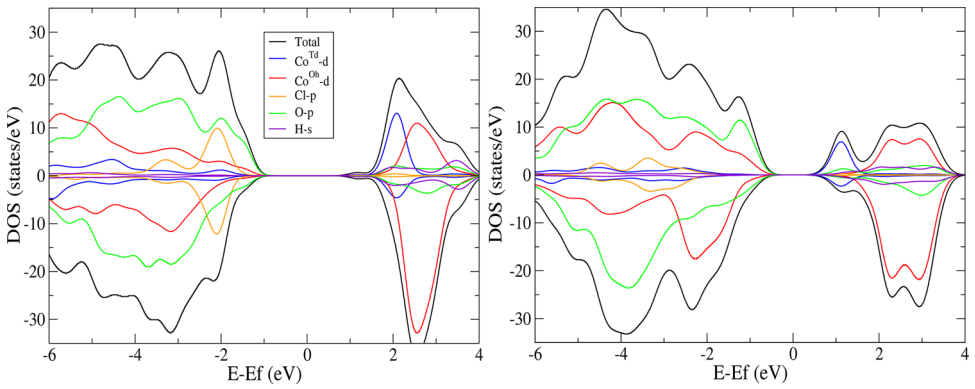

Figure 7. Total and projected density of states for a single layer of the α-hydroxide with n = 8 (left panel) and n = 15 (right panel).

all supercells examined in our calculations, the magnetic coupling between the two types of cobalt ions was always found to be antiferromagnetic, so that the relative distribution of Co^{Td} does not seem to affect the magnetic ordering.

Once the key features of the isolated layers were established, we focused on the description of a more realistic 3D scenario. First, the magnetic coupling between the planes was examined for a supercell model containing stacked infinite layers with m = 2 and variable y. The interlayer distance d_{00l} remains practically invariant as a function of the Co^{Td} concentration, as shown in Table 4.

Table 4. Optimized Lattice Parameters, in Å, for the α-Hydroxide Crystal with m = 2 and y = 0 and Different Tetrahedral Cobalt Fractions[a]

n	d_{00l}
3	7.92
8	7.95
15	7.93
exp ($n \approx 8$)	8.0016

[a]The experimental values correspond to Rietveld refinements[9].

For all n examined in this work, the ground state turned out to be antiferromagnetic. The relative energies of the FM states are compiled in Table 5 (see SI for alternative magnetic configurations). Independent of the concentration of tetrahedral sites, the different layers are antiferromagnetically coupled, where the magnetic moments of Co^{Oh} ions belonging to a layer are anti-aligned with respect to the Co^{Oh} ions belonging to the adjacent one. The same kind of coupling is found for the magnetic moment of Co^{Td} sites. Figure 8 schematically depicts the magnetic ground state of these systems.

Table 5. Energy of the FM Configuration Relative to the Ground (AF) State, in meV/Co, for the 3D Crystal with Different Proportions of Tetrahedric Cobalt Sites

magnetic state	ΔE/Co (n = 3)	ΔE/Co (n = 8)	ΔE/Co (n = 15)
FM	2	5	8

These calculations are consistent with the low-temperature neutron diffraction experiments reported by Neilson et al. for disordered α phases.[25] Based on a mean field theory analysis of magnetic susceptibility measurements, they concluded that the two types of cobalt ions in the layers present AF coupling. Neutron diffraction measurements[25] on deuterated samples

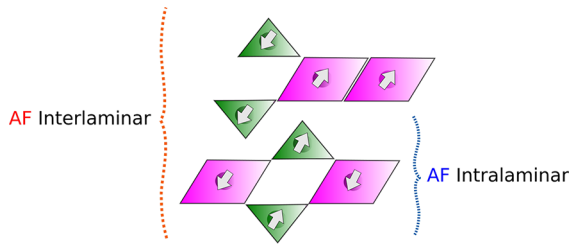

Figure 8. Schematic view of the intra and interlaminar magnetic coupling, illustrated for a model of the $[Co^{Oh}{}_8Co^{Td}{}_2(OH)_{18}Cl_2]_2$ solid.

with a tetrahedral cobalt concentration of 0.4 confirm this magnetic behavior from the occurrence of a characteristic diffraction peak at a distance of 16.31 Å employing a wave vector k = (0,0,1/2). This distance is equal to twice the value of the d_{00l} parameter, implying that the magnetic cell has two layers, in contrast to the atomic unit cell obtained by Sasaki and co-workers[9] by means of Rietveld refinement, indexed with three layers.

The electronic structure is not significantly affected by the interlayer interactions. In the stacked solid with n = 3 at the equilibrium distance, the band gap is 2.3 eV (Figure 9). The DOS profile in the proximity of the Fermi level receives a larger contribution from the oxygen atoms in the valence states, although the previously noticed degeneration of the d orbitals remains.

The interlayer space may accommodate a variable number of water molecules, depending on the ambient humidity or exposure to an aqueous phase. In principle, the hydration degree should strongly determine the interlayer distance. To investigate this dependence, we optimized the d_{00l} parameter for different water contents. The results are presented in Figure 10. On the left panel, it is seen that the expansion D caused by the insertion of interlayer solvent, defined as the increase in separation with respect to the dehydrated structure, is more pronounced the higher the content of tetrahedral centers. It must be recalled that these sites lie out of the plane, occupying part of the interlayer volume. Thus, the space available for guest molecules strongly varies in the present family of $[Co^{Oh}{}_nCo^{Td}{}_2(OH)_{2n+2}Cl_2]_2{\cdot}(H_2O)_{y\cdot 2}$ supercells. If the water content is normalized with respect to the empty interlayer space, for example, as the amount of H_2O per Co^{Oh} site, then the expansion D displays the same trend in all systems (Figure 10, right panel). This structural response to hydration, both in interlayer expansion and water configuration, is similar to that observed in related families of layered materials.[34,35]

DOI: 10.1021/acs.inorgchem.7b03231
Inorg. Chem. XXXX, XXX, XXX−XXX

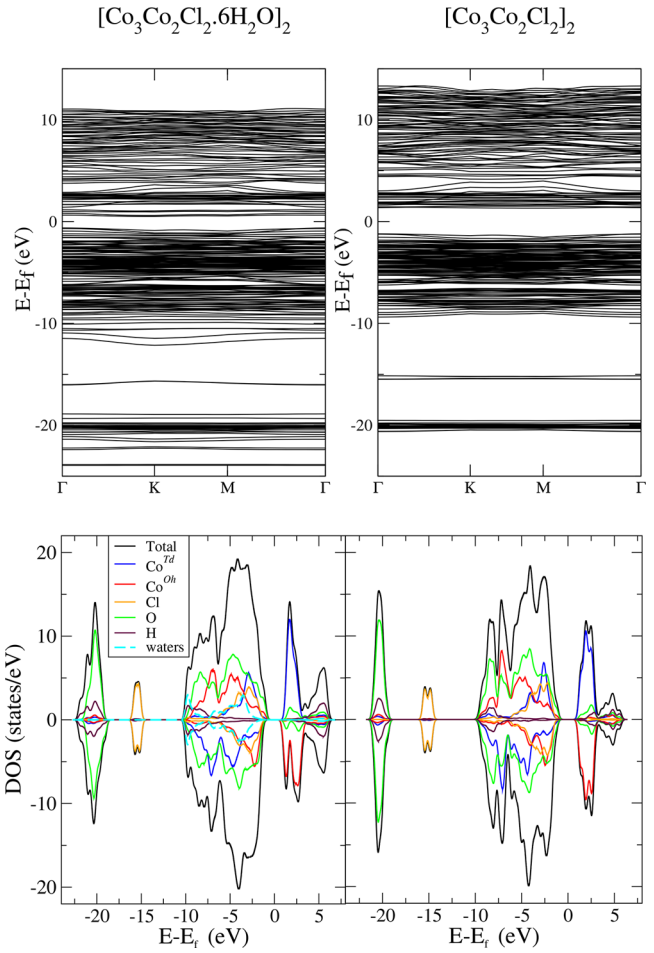

Figure 9. Band structure (top) and projected density of states (bottom) for the α-hydroxide (n = 3) with (left) and without (right) interlayer water molecules.

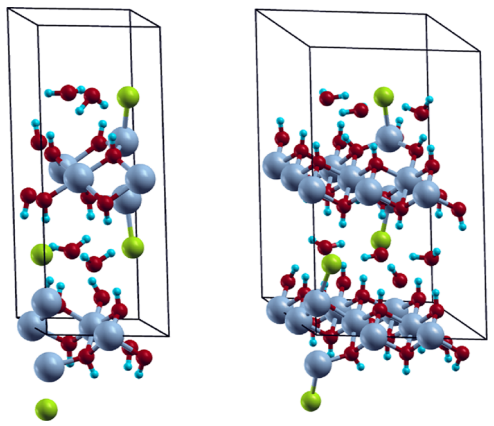

Figure 11. Optimized structures of the supercells with n = 3 and n = 8 containing, respectively, four and six water molecules.

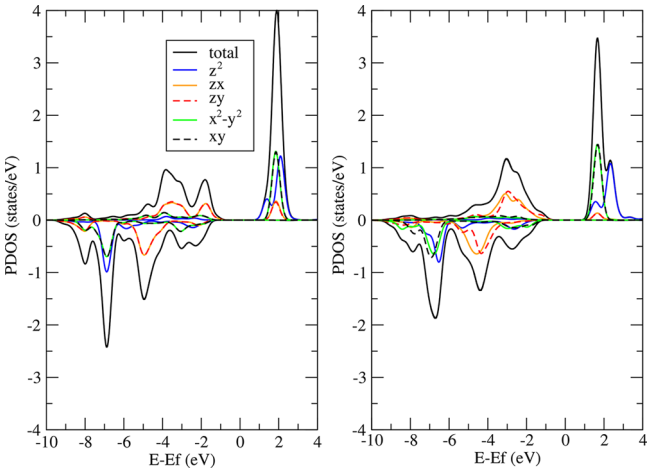

Figure 12. Projected density of states for Co d-orbitals in the α-hydroxide (n = 3), with (left) and without (right) interlayer water molecules.

Interestingly, the presence of interstitial water seems to have a major effect on the electronic structure of the solid. Some representative optimized structures are depicted in Figure 11. Upon interaction of the H_2O molecules with the highly exposed chlorides, a marked distortion of the Co^{Td} environment results in the rupture of the d degeneracy, evinced in Figure 12. The overall effect of hydration over the electronic structure of the solid can be observed in Figure 9, being the main feature the diminished gap value for the hydrated array, which drops to 1.1 eV when n = 3. An inspection of the atomic charges (Table 6) reveals a depletion of electron density on chloride atoms, polarized by their interactions with H_2O, which drives a charge transfer to Co^{Td} and, to a lesser extent, to Co^{Oh}. This charge density redistribution arising from chlorine polarization by water has a significant impact on E_{gap}, by filling the d levels around the Fermi energy.

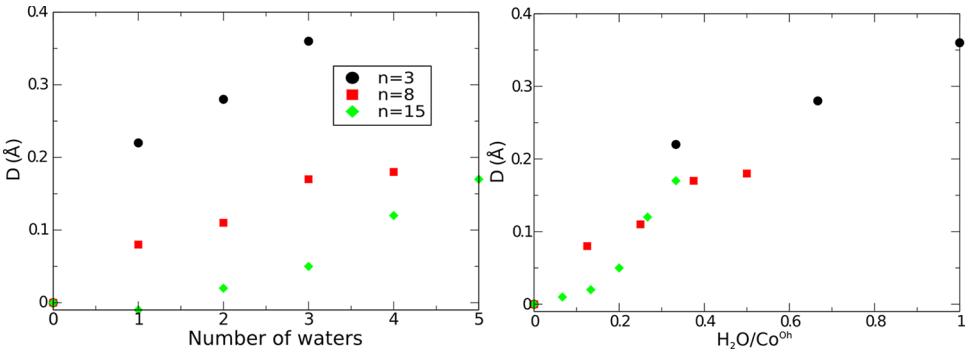

Figure 10. Interlayer expansion, D, as a function of the content of water molecules, for different concentrations of tetrahedral cobalt sites. The right panel depicts the same data, but the water content is normalized per Co^{Oh} site.

DOI: 10.1021/acs.inorgchem.7b03231
Inorg. Chem. XXXX, XXX, XXX−XXX

Table 6. Electronic Populations Based on Löwdin Analysis for Cl, Co^{Td}, and Co^{Oh} Atoms in the n = 3 Supercell, with and without Interlayer Water Molecules

	Cl	Co^{Td}	Co^{Oh}
dried	7.57	7.82	7.80
hydrated	6.92	8.05	7.81

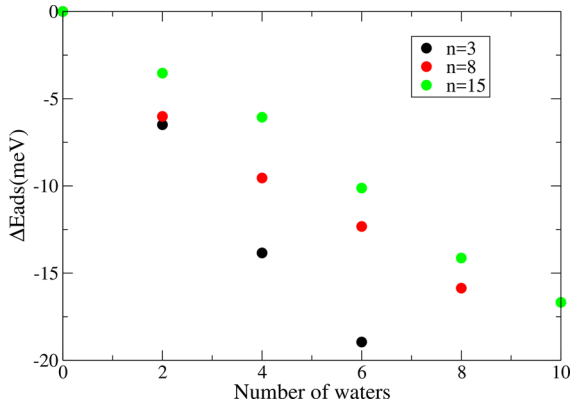

Figure 13. Hydration energy for the different supercells, as a function of the number of water molecules. Note that this number corresponds to a supercell of two layers.

Figure 13 presents the hydration energy of the solid as a function of the number of water molecules in the interlayer space. This energy corresponds to the process:

$$[Co^{Oh}{}_n Co^{Td}{}_2(OH)_{2n+2}Cl_2]_2 + s(H_2O) \rightarrow [Co^{Oh}{}_n Co^{Td}{}_2(OH)_{2n+2}Cl_2]_2 \cdot (H_2O)_s$$

The Figure reflects a strong stabilization associated with the incorporation of water. The energy values should be regarded as merely indicative, since they come from optimized structures which are only local minima in the complex potential energy surface corresponding to the hydrated crystal. However, the magnitude of the energetic decrease as a function of water content is eloquent enough to attest a large thermodynamic stabilization resulting from the adsorption of H_2O. The optimized structures show that the hydrogen-bond network arising from the water molecules significantly contributes to the interlayer forces.

CONCLUSIONS

We have presented here, to the best of our knowledge, the first theoretical study of the magnetic order, and of the electronic and atomic structure, of cobalt α hydroxides on the basis of DFT+U calculations. The intra and interlayer magnetic couplings resulting from the simulations are consistent with neutron diffraction experiments and susceptibility measurements. Furthermore, our results show that, in comparison to the β-phase, the α hydroxides exhibit a reduced band gap for an intermediate fraction of Co^{Td}, corresponding to the formula $[Co^{Oh}{}_{15}Co^{Td}{}_2(OH)_{32}Cl_2]$, arising from the contribution of the tetrahedral cobalt density to the Fermi level. In this case E_{gap} drops to around 1.4 eV, significantly below the value of 2 eV corresponding to the β-hydroxide. This band gap decrease is exacerbated by the presence of interstitial water molecules, thanks to the polarization of the chloride ligands. The overall effect of the intralayer H_2O molecules is a charge transfer to the tetrahedral cobalt sites which provokes a further closure of the band gap. On the other hand, the hydration degree has an impact on the interlayer distance d_{001} and at the same time significantly contributes to the stability of the solid thanks to a hydrogen-bond network which keeps the layers together. This peculiar sensitivity to the presence of water both in terms of structural and electrical properties can be regarded as a very interesting asset with possible applications in sensor or responsive materials. As already mentioned, this investigation constitutes the first approach to the electronic and structural properties of α-$Co(OH)_2$ from a theoretical viewpoint, emphasizing the power of DFT+U to provide insights and to complement the experimental characterization of this family of layered cobalt compounds.

ASSOCIATED CONTENT

Supporting Information

The Supporting Information is available free of charge on the ACS Publications website at DOI: 10.1021/acs.inorgchem.7b03231.

Details on the calculation of the magnetic coupling constants, the relative energies for various additional configurations, the effect of U on the magnetic state, and an analysis of the role of the halogen on the mangetic interaction (PDF)

AUTHOR INFORMATION

Corresponding Authors

*E-mail: hunt@tandar.cnea.gov.ar.
*E-mail: damian@qi.fcen.uba.ar.

ORCID

Matías Jobbagy: 0000-0002-6860-341X
Damián A. Scherlis: 0000-0002-0588-287X

Notes

The authors declare no competing financial interest.

ACKNOWLEDGMENTS

D.H. acknowledges CONICET for a postdoctoral fellowship. D.H. dedicates this work to lovely MICIELA. We thank the allocation of computational time in the HPC Cluster CONICET-Rosario. This study has been supported by grants of ANPCYT/PICT 2012-2292 and UBACYT 20020160100124BA.

REFERENCES

(1) Kurmoo, M. Magnetic metal-organic frameworks. *Chem. Soc. Rev.* **2009**, *38*, 1353−1379.
(2) Zadrozny, J. M.; Liu, J.; Piro, N. A.; Chang, C. J.; Hill, S.; Long, J. R. Slow magnetic relaxation in a pseudotetrahedral cobalt(II) complex with easy-plane anisotropy. *Chem. Commun.* **2012**, *48*, 3927−3929.
(3) Mondal, A.; Durdevic, S.; Chamoreau, L.-M.; Journaux, Y.; Julve, M.; Lisnard, L.; Lescouezec, R. A cyanide and hydroxo-bridged nanocage: a new generation of coordination clusters. *Chem. Commun.* **2013**, *49*, 1181−1183.
(4) Rabu, P.; Angelov, S.; Legoll, P.; Belaiche, M.; Drillon, M. Ferromagnetism in triangular cobalt(II) layers: comparison of cobalt dihydroxide and cobalt nitrate hydroxide ($Co_2(NO_3)(OH)_3$). *Inorg. Chem.* **1993**, *32*, 2463−2468.
(5) Kurmoo, M.; Kumagai, H.; Hughes, S. M.; Kepert, C. J. Reversible Guest Exchange and Ferrimagnetism (T_C = 60.5 K) in a Porous Cobalt(II)-Hydroxide Layer Structure Pillared with trans-1,4-Cyclohexanedicarboxylate. *Inorg. Chem.* **2003**, *42*, 6709−6722.
(6) Schwenzer, B.; Roth, K. M.; Gomm, J. R.; Murr, M.; Morse, D. E. Kinetically controlled vapor-diffusion synthesis of novel nanostruc-

DOI: 10.1021/acs.inorgchem.7b03231
Inorg. Chem. XXXX, XXX, XXX−XXX

tured metal hydroxide and phosphate films using no organic reagents. *J. Mater. Chem.* **2006**, *16*, 401−407.
(7) Kurmoo, M. Ferrimagnetism in dicarboxylate-bridged cobalt hydroxide layers. *J. Mater. Chem.* **1999**, *9*, 2595−2598.
(8) Du, Y.; O'Hare, D. Synthesis, Morphology, Structure, and Magnetic Characterization of Layered Cobalt Hydroxyisocyanates. *Inorg. Chem.* **2008**, *47*, 3234−3242.
(9) Ma, R.; Liu, Z.; Takada, K.; Fukuda, K.; Ebina, Y.; Bando, Y.; Sasaki, T. Tetrahedral Co(II) Coordination in α-Type Cobalt Hydroxide: Rietveld Refinement and X-ray Absorption Spectroscopy. *Inorg. Chem.* **2006**, *45*, 3964−3969.
(10) Hawthorne, F.; Sokolova, E. Simonkolleite, $Zn_5(OH)_8Cl_2(H_2O)$, a decorated interrupted-sheet structure of the form $[M\phi_2]_4$. *Can. Mineral.* **2002**, *40*, 939−946.
(11) Neilson, J. R.; Schwenzer, B.; Seshadri, R.; Morse, D. E. Kinetic Control of Intralayer Cobalt Coordination in Layered Hydroxides: $Co_{1-0.5x}{}^{oct}Co_x{}^{tet}(OH)_2(Cl)_x(H2O)_2$. *Inorg. Chem.* **2009**, *48*, 11017−11023.
(12) Smith, M. B.; Page, K.; Siegrist, T.; Redmond, P. L.; Walter, E. C.; Seshadri, R.; Brus, L. E.; Steigerwald, M. L. Crystal Structure and the Paraelectric-to-Ferroelectric Phase Transition of Nanoscale $BaTiO_3$. *J. Am. Chem. Soc.* **2008**, *130*, 6955−6963.
(13) Petkov, V.; Billinge, S. J. L.; Heising, J.; Kanatzidis, M. G. Application of Atomic Pair Distribution Function Analysis to Materials with Intrinsic Disorder. Three-Dimensional Structure of Exfoliated-Restacked WS_2: Not Just a Random Turbostratic Assembly of Layers. *J. Am. Chem. Soc.* **2000**, *122*, 11571−11576.
(14) Gateshki, M.; Hwang, S.-J.; Park, D. H.; Ren, Y.; Petkov, V. Structure of Exfoliated Titanate Nanosheets Determined by Atomic Pair Distribution Function Analysis. *Chem. Mater.* **2004**, *16*, 5153−5157.
(15) Neilson, J.; Kurzman, J.; Seshadri, R.; Morse, D. Cobalt Coordination and Clustering in α-$Co(OH)_2$ Revealed by Synchrotron X-ray Total Scattering. *Chem. - Eur. J.* **2010**, *16*, 9998−10006.
(16) Giannozzi, P.; et al. QUANTUM ESPRESSO: a modular and open-source software project for quantum simulations of materials. *J. Phys.: Condens. Matter* **2009**, *21*, 395502−395521.
(17) Perdew, J. P.; Burke, K.; Ernzerhof, M. Generalized Gradient Approximation Made Simple. *Phys. Rev. Lett.* **1996**, *77*, 3865−3868.
(18) Anisimov, V. I.; Zaanen, J.; Andersen, O. K. Band theory and Mott insulators: Hubbard U instead of Stoner I. *Phys. Rev. B: Condens. Matter Mater. Phys.* **1991**, *44*, 943−954.
(19) Wang, L.; Maxisch, T.; Ceder, G. Oxidation energies of transition metal oxides within the GGA + U framework. *Phys. Rev. B: Condens. Matter Mater. Phys.* **2006**, *73*, 195107.
(20) Dalverny, A.; Filhol, J.; Lemoigno, F.; Doublet, M. Interplay between Magnetic and Orbital Ordering in the Strongly Correlated Cobalt Oxide: A DFT+U Study. *J. Phys. Chem. C* **2010**, *114*, 21750−21756.
(21) Chen, J.; Wu, X.; Selloni, A. Electronic structure and bonding properties of cobalt oxide in the spinel structure. *Phys. Rev. B: Condens. Matter Mater. Phys.* **2011**, *83*, 245204.
(22) Chen, J.; Selloni, A. First Principles Study of Cobalt (Hydr)oxides under Electrochemical Conditions. *J. Phys. Chem. C* **2013**, *117*, 20002−20006.
(23) Grimme, S. Semiempirical GGA-type density functional constructed with a long-range dispersion correction. *J. Comput. Chem.* **2006**, *27*, 1787−1799.
(24) Barone, V.; Casarin, M.; Forrer, D.; Pavone, M.; Sambi, M.; Vittadini, A. Role and effective treatment of dispersive forces in materials: Polyethylene and graphite crystals as test cases. *J. Comput. Chem.* **2009**, *30*, 934−939.
(25) Neilson, J.; Morse, D.; Melot, B.; Shoemaker, D.; Kurzman, J.; Seshadri, R. Understanding complex magnetic order in disordered cobalt hydroxides through analysis of the local structure. *Phys. Rev. B: Condens. Matter Mater. Phys.* **2011**, *83*, 094418.
(26) Himmetoglu, B.; Floris, A.; de Gironcoli, S.; Cococcioni, M. Hubbard-corrected DFT energy functionals: The LDA+U description of correlated systems. *Int. J. Quantum Chem.* **2014**, *114*, 14−49.
(27) Freysoldt, C.; Grabowski, B.; Hickel, T.; Neugebauer, J.; Kresse, G.; Janotti, A.; Van de Walle, C. G. First-principles calculations for point defects in solids. *Rev. Mod. Phys.* **2014**, *86*, 253−305.
(28) Kulik, H. J.; Cococcioni, M.; Scherlis, D. A.; Marzari, N. Density Functional Theory in Transition-Metal Chemistry: A Self-Consistent Hubbard *U* Approach. *Phys. Rev. Lett.* **2006**, *97*, 103001.
(29) Hunt, D.; Garbarino, G.; Rodriguez-Velamazan, J. A.; Ferrari, V.; Jobbagy, M.; Scherlis, D. A. The magnetic structure of β-cobalt hydroxide and the effect of spin-orientation. *Phys. Chem. Chem. Phys.* **2016**, *18*, 30407−30414.
(30) Lloret, F.; Julve, M.; Cano, J.; Ruiz-García, R.; Pardo, E. Magnetic properties of six-coordinated high-spin cobalt(II) complexes: Theoretical background and its application. *Inorg. Chim. Acta* **2008**, *361*, 3432−3445.
(31) The total magnetization M_{tot} is defined according to the following formula:

$$M_{tot} = -\mu_B \int (\rho_\alpha(\mathbf{r}) - \rho_\beta(\mathbf{r}))d\mathbf{r}$$

where μ_B is the Bohr magneton, and ρ_α (**r**) and ρ_β(**r**) are the up and down electronic densities. In the supercell with $n = 3$, for example, the magnetic ground state involves three Co^{Oh} spin-up centers and two Co^{Td} spin-down centers. Hence, a value of $M_{tot} = 3\ \mu_B$ is consistent with high-spin Co(II) ions, exhibiting three unpaired electrons each.
(32) Goodenough, J. *Magnetism and the Chemical Bond*; Interscience Publisher: New York, 1963.
(33) Kahn, O. *Molecular Magnetism*; VCH Publishers Inc.: New York, 1993.
(34) Iyi, N.; Fujii, K.; Okamoto, K.; Sasaki, T. Factors influencing the hydration of layered double hydroxides (LDHs) and the appearance of an intermediate second staging phase. *Appl. Clay Sci.* **2007**, *35*, 218−227.
(35) Jobbagy, M.; Iyi, N. Interplay of Charge Density and Relative Humidity on the Structure of Nitrate Layered Double Hydroxides. *J. Phys. Chem. C* **2010**, *114*, 18153−18158.

DOI: 10.1021/acs.inorgchem.7b03231
Inorg. Chem. XXXX, XXX, XXX−XXX